Indian Journal of Radio & Space Physics
Vol. 17, April 1988, pp. 63-68

Vertical Distribution of Water Vapour over Hyderabad

A JAYARAMAN & B H SUBBARAYA
Physical Research Laboratory, Ahmedabad 380009

Received 16 *April* 1987; *revised received* 25 *November* 1987

Under the Indian Middle Atmosphere Program (IMAP), a balloon carrying PRL's sun-tracking multichannel photometer was launched from Hyderabad Balloon Facility on 22 Oct. 1985. Radiation measurements were made in the wavelength regions of 215, 290, 310, 450, 600 and 800 nm. The vertical distributions of zone, aerosol and water vapour concentrations are derived. The data analysis technique used and the results obtained on the atmospheric water vapour concentration are presented. The water vapour mixing ratio profile thus obtained in the altitude region of 10-31 km shows a broad minimum (called hygropause) around 16 km with a mixing ratio value of 2.82 ppmv.

1 Introduction

Water vapour (H_2O) concentrations in the low altitude region (up to about 8 km) are regularly being measured by the standard meteorological balloon soundings and studied[1]. Apart from the climatological importance, water vapour at higher altitudes is found to play an important role in atmospheric chemistry[2], growth of aerosol particles[3], and formation of ion clusters[4]. For example, H_2O reacts with $O(^1D)$ to form hydroxyl (OH) radical. The OH radicals involve in the chemistry of ozone destruction along with NO_X and ClO_X families at stratospheric and tropospheric levels. Moreover, the atmospheric water vapour over the tropical region plays a major role in the global water budget. It is believed[5,6] that the moist air rises upwards through tropical tropopause and spreads polewards. However, the in situ measurements of H_2O at tropical tropospheric and stratospheric altitudes are sparse[7].

The techniques commonly used for the measurements of water vapour are UV fluorescence[8], Frost-point hygrometry[9], and IR emission radiometry[10]. This paper describes the in situ measurement of water vapour over the tropical site, Hyderabad (17.5°N) using photometric technique. Apart from the strong absorption bands of water vapour in the far infrared region, water vapour also has three weak but distinct absorption bands in the wavelength region of 690-1000 nm designated as α, 0.8 μm and $\rho\sigma\tau$ bands[11]. Even though these bands are comparatively weak, the attenuation of the solar radiation due to these bands can be measured[12] for long atmospheric path-lengths corresponding to large solar zenith angles. In the present work, the attenuation of the direct solar radiation due to 0.8 μm absorption band of H_2O is measured for solar zenith angles ranging from 83° to 68° corresponding to a balloon altitude of 10-31 km.

2 Experimental Details

Under the Indian Middle Atmosphere Program (IMAP), a 29,262 m^3 balloon carrying PRL's sun-tracking multichannel photometer and conductivity probes, was launched from Hyderabad Balloon Facility on 22 Oct. 1985 at 0611 hrs. The balloon reached the ceiling altitude of about 31.5 km at 0750 hrs (Fig. 1). After a float period of about

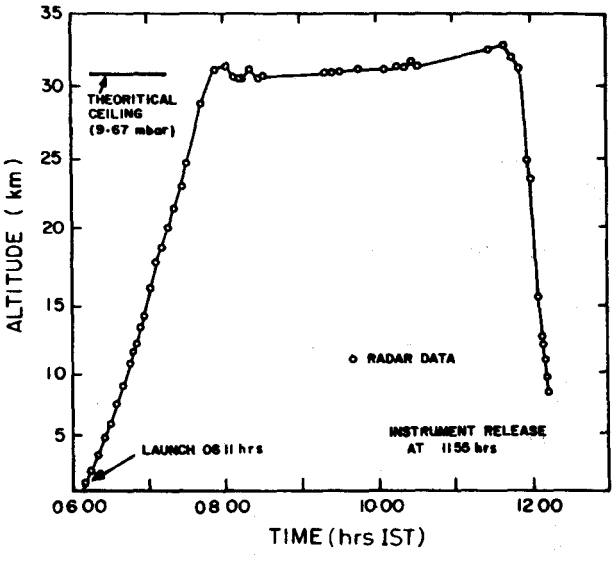

Fig. 1—Trajectory of the balloon launched from Hyderabad Balloon Facility on 22 Oct. 1985

4 hr, the instrument was released by telecommand and recovered in good condition.

The sun-tracking multichannel photometer is essentially a six-channel photometer, tracking the sun in the vertical direction and scanning in the azimuthal direction, ± 90° with respect to sun. For aerosol measurements, information on the intensity of the direct solar radiation and the angular distribution of the scattered intensity is necessary. In the present flight, the scanning time of the photometers was 15 s in one direction.Taking the typical balloon ascent speed as 250 m/min, 16 data sets were obtained in every kilometre. This corresponds to a vertical resolution of about 62.5 m. Suitable combinations of phototubes/diodes and interference filters were used to measure the radiation intensities in the six wavelength regions, viz. 215, 290, 310, 450, 600 and 800 nm. Table 1 gives the centre wavelength (λ_0), transmission (T) and bandwidth (full width at half maximum, FWHM) of the interference filters used. The currents from the photometers were fed to logarithmic amplifiers, having a dynamic range of more than 6 orders of magnitude. The amplified signals were digitized and transmitted to ground station, using PCM/FM telemetry system. More detailed description of the instrument is available elsewhere[13].

3 Data Analysis

Out of the six channels, data on the vertical distribution of solar radiation in the 215 nm were used to study the photodissociation processes in the tropospheric and stratospheric levels involving molecular oxygen and other minor constituents. The 290 and 310 nm channels fall in the Hartley bands of ozone absorption. The attenuation profiles derived from the direct solar radiation measurements in these two wavelength regions were used to obtain the ozone concentration profile up to the balloon ceiling altitude. The 450 nm channel was relatively free from absorption due to any atmospheric gases except nitrogen dioxide (NO_2). However, the absorption due to NO_2 was about an order of magnitude less than the scattering due to air molecules and aerosols at this wavelength. The data on the intensity of the direct solar radiation and the angular distribution of the scattered radiation at different altitude levels corresponding to 450 nm were analyzed to obtain the vertical distribution of aerosol concentration and size distribution function. The 600 nm channel falls in the Chappuis band of ozone absorption. The ozone concentration values derived from 290 and 310 nm channels were used to estimate the attenuation due to ozone in the 600 nm band and subtracted from the total attenuation to derive the aerosol attenuation coefficients. This information was used to validate the results obtained from 450 nm. The 800 nm channel was influenced by ozone absorption (Chappuis band), H_2O absorption (0.8μm band), and scattering processes. The aerosol attenuation coefficients calculated using the aerosol concentrations and size distribution function and the ozone absorption coefficients were subtracted from the total attenuation to estimate the absorption due to water vapour alone. The data analysis procedure for obtaining ozone concentrations, aerosol attenuation coefficient and water vapour concentrations is described below.

Table 1—Characteristics of the Interference Filters Used in the Experiment

Filter No.	λ_0 nm	T %	FWHM nm
215	214	9.4	11.0
290	291	22.0	22.0
310	312	16.0	17.0
450	451	43.0	8.5
600	599	44.0	7.5
800	797	57.0	12.5

3.1 Ozone

Fig. 2 shows the 10-point running average of the 290 and 310 nm photometer currents with an altitude resolution of about 0.6 km. The output currents are plotted against time. The correspond-

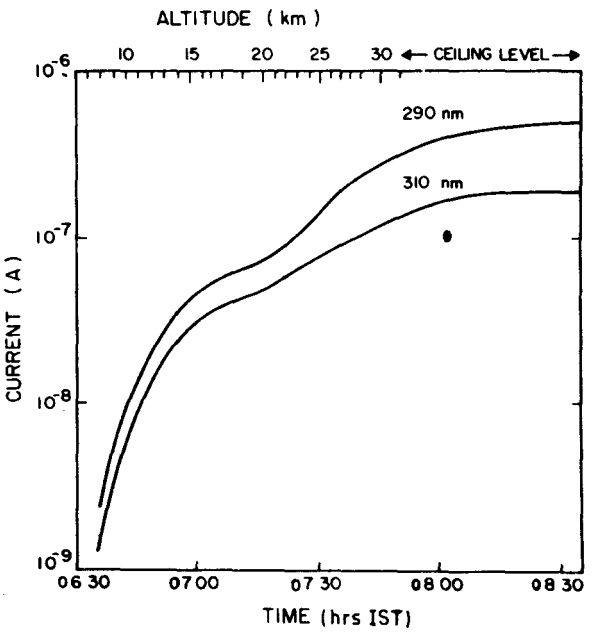

Fig. 2—Photometer currents smoothed using 10-point running average

ing balloon altitudes are also shown. The higher current measured by the 290 nm channel than that by the 310 nm channel is due to the higher transmission and larger bandwidth of the interference filter used (see Table 1). The increase in the outputs at the balloon ceiling altitude level is due to the decrease in solar zenith angle with increasing time.

Ozone number densities are calculated as a function of altitude using the relation

$$n_{O_3}(Z) = \frac{dI(Z)}{I(Z) \cdot dZ \cdot F(Z,\chi)\, \sigma_{eff}(Z)} \quad \ldots (1)$$

where $I(Z)$ is the measured photometer current, $F(Z, \chi)$ the optical depth factor, and $\sigma_{eff}(Z)$ the effective absorption cross-section of ozone. Ozone concentrations are estimated separately for the two channels and the mean concentration profile is obtained. However, more weightage is given to the 310 nm at lower altitudes and to 290 nm at higher altitudes. Fig. 3 shows the obtained ozone concentration profile over Hyderabad. Comparison of the present ozone profile with that of earlier result[14] obtained over Hyderabad on 27 Mar. 1985 shows that the peak ozone level is at the same altitude level of 23-24 km region with the same ozone concentration of 4.6×10^{12} molecules/cc. However, the marked minimum in the concentration value found at 16 km in the experiment conducted on 27 Mar. 1985 is not found in the present case. Ozone absorption coefficient is calculated using the relation

$$\beta_{O_3}(Z,\lambda) = n_{O_3}(Z) \cdot \sigma_{O_3}(\lambda) \cdot 10^5 \quad \ldots (2)$$

where $\sigma_{O_3}(\lambda)$ is the ozone absorption cross-section[15].

3.2 Aerosol

Data on the direct solar radiation and the angular distribution of the scattered radiation at different atmospheric levels are inverted to obtain the aerosol number density and the slope in the power law size distribution curve. Results on the obtained aerosol parameters are presented elsewhere[16].

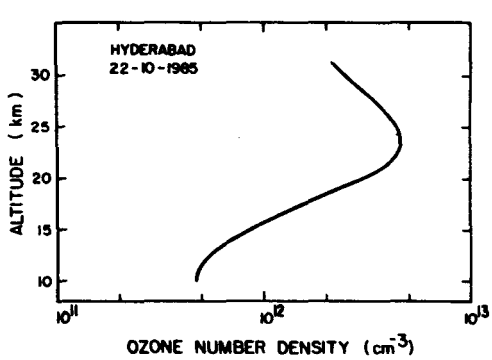

Fig. 3—Ozone concentration profile obtained over Hyderabad on 22 Oct. 1985

Aerosol attenuation coefficients are calculated using the relation

$$\beta_{aerosol}(Z) = 2\pi \frac{C}{\ln 10} \left(\frac{2\pi}{\lambda}\right)^{\nu-2} \int_0^{\pi} \eta(\lambda,\theta) \sin\theta \, d\theta \quad \ldots (3)$$

where

$$C = \frac{\eta_{aerosol}(Z)}{0.434 \int_{r_1}^{r_2} dr/r^{(\nu+1)}} \quad \ldots (4)$$

$\eta(\lambda, \theta)$ is the Mie angular function corresponding to a refractive index of 1.5. Detailed description of the estimation of aerosol attenuation coefficient is available elsewhere[17]. It should be noted here that the Rayleigh scattering contribution decreases with increasing wavelength, in accordance with $1/\lambda^4$ law. However, aerosol scattering is less wavelength dependent. For power law size distribution, the wavelength dependence of aerosol scattering takes the form

$$\frac{1}{\lambda^{\nu-2}} \quad \ldots (5)$$

Therefore, aerosol scattering becomes more important than Rayleigh scattering at higher wavelengths[18].

3.3 Rayleigh Scattering

The Rayleigh scattering coefficients are calculated using the relation

$$\beta_{air}(Z,\lambda) = n_{air}(Z) \cdot \sigma_{air}(\lambda) \cdot 10^5 \quad \ldots (6)$$

where $n_{air}(Z)$ is the number density of air molecules expressed per cm^3 at altitude Z and $\sigma_{air}(\lambda)$ is the Rayleigh scattering cross-section expressed in cm^2. In the present computation, the air density values are taken from the *US Standard Atmosphere* 1976 (Ref. 19) for 15°N and Rayleigh scattering cross-section values are those as given by Penndorf[20].

3.4 Computations of H_2O Concentrations

The measured photometer current corresponding to 800 nm channel is smoothed using 10-point

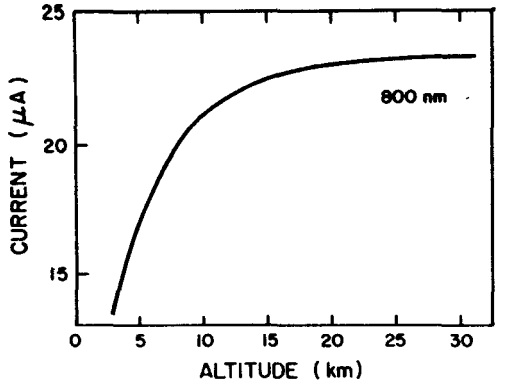

Fig. 4—Photometer current corresponding to 800 nm

running average and plotted against altitude in Fig. 4. The sharp rise in the current from 3 to 10 km altitude is due to higher water vapour concentrations as well as longer optical path-lengths. The increase in the photometer current at higher altitudes ($Z > 20$ km) is found to be small due to decrease in the total attenuation with increasing altitude. However, onboard digitization of the data, subsequent recording on digital magnetic tape and computer-based data analysis, make it possible to measure any small increase in the output values to an accuracy of 0.001%. Moreover, since the log of the output is measured, the difference in the two successive values ($\mathrm{d}[\log I] = \mathrm{d}I/I$) directly gives the total attenuation at any altitude.

Fig. 5 shows the estimated height profiles of the ozone absorption, Rayleigh and aerosol scattering coefficients. The Rayleigh scattering coefficient is found to be higher than ozone absorption and aerosol scattering at all altitudes below about 25 km. Ozone absorption becomes comparable to Rayleigh scattering above the ozone peak level. The low aerosol scattering coefficients obtained on 22 Oct. 1985 is believed to represent the background aerosol concentrations, not influenced by any volcanic eruption. From the total attenuation coefficient derived from 800 nm channel output, the contributions due to ozone absorption, aerosol and air molecule scattering are subtracted to obtain the absorption coefficient (β_{H_2O}) due to water vapour. The H_2O mixing ratio in parts per million by volume (ppmv) is obtained using the relation

$$H_2O \text{ mixing ratio } (Z) = \frac{\beta_{H_2O} \cdot 10}{\sigma'_{H_2O} \cdot n_{air}(Z)} \qquad \ldots (7)$$

σ'_{H_2O} is the weighted average of the H_2O absorption cross-sections expressed in cm^2 derived from the absorptance values published by Tanaka *et*

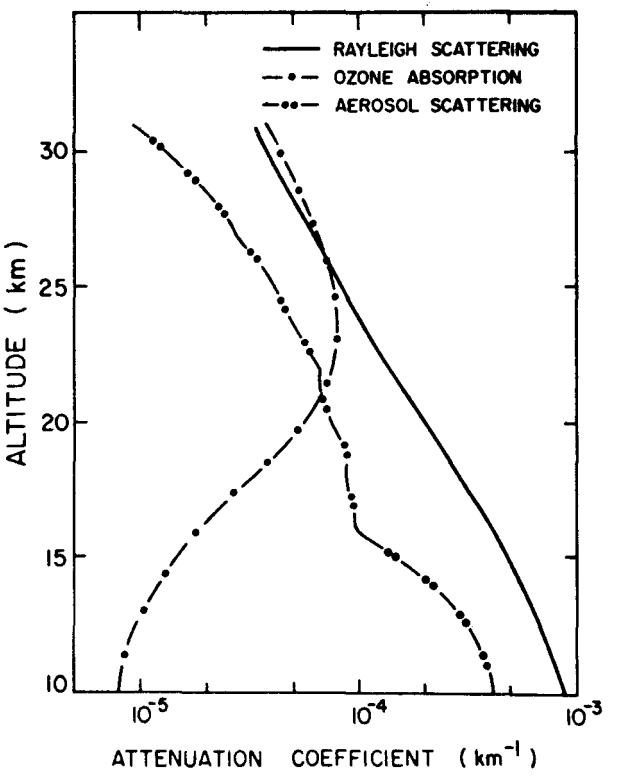

Fig. 5—Altitude variations of the computed attenuation coefficients for 800 nm corresponding to Rayleigh scattering, ozone absorption and aerosol scattering

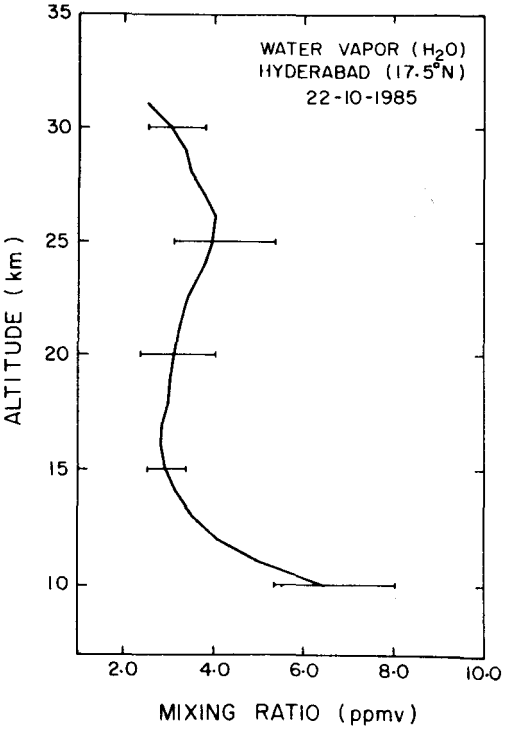

Fig. 6—Water vapour mixing ratio profile obtained over Hyderabad on 22 Oct. 1985

al.[11] The weighted average of σ_{H_2O} is taken for the effective bandwidth of the 800 nm channel.

4 Results and Discussion

Fig. 6 shows the obtained water vapour mixing ratio in ppmv from 10 to 31 km; for clarity, error bars are shown at every 5-km altitude. Mixing ratio values are also tabulated in Table 2 along with the estimated uncertainties in the derived values for every kilometre. The error is due to the uncertainties in the derived ozone and aerosol concentration values. The obtained mixing ratio values are found to vary between 6.42 ppmv at 10 km and 2.51 ppmv at 31 km with a minimum around 16 km. The minimum water vapour encountered above the tropical tropopause level was referred to as hygropause by Kley *et al.*[21] The meteorological sounding (radiosonde) made on the same day (22 Oct. 1985) over Hyderabad shows the tropopause at 15.3 km with a temperature of −79.4°C. Mean of several water vapour profiles obtained over the tropical region shows a water vapour mixing ratio of 3.4 ppmv at about 18.5 km (Ref. 22). The corresponding mean temperature profile shows the tropopause level at about 17 km. In the present measurement, we observed the hygropause in the 16-17 km region with a water vapour mixing ratio of 2.82 ± 0.45 ppmv.

Above the hygropause level the H_2O mixing ratio is found to increase and reaches a broad maximum around 26 km. Contrary to the earlier belief of nearly constant water vapour mixing ratios in the stratosphere and mesosphere, several recent observations[22,23] have also shown an increase in the mixing ratio values above the hygropause level. This increase is now believed to be due to the production of H_2O through methane (CH_4) oxidation at stratospheric levels[24]. However, simultaneous measurements[25,26] of H_2O and CH_4 show that the increase in H_2O concentration with height is larger than that which would be expected from CH_4 oxidation alone. Also, stratospheric H_2O has long chemical lifetime, of the order of a few years in the lower stratosphere, and hence the observed variations in the mixing ratio profile can be related to the transport processes.

The destruction processes of H_2O include photolysis by UV radiation:

$$H_2O + h\nu(\lambda < 200\ \text{nm}) \rightarrow H + OH$$

and the reaction of H_2O with $O(^1D)$:

$$H_2O + O(^1D) \rightarrow 2OH$$

Due to the lack of data above 31 km, it is not very clear whether the observed decrease in the H_2O mixing ratio above about 28 km is due to the destruction of H_2O or is a transient feature, influenced by the transport processes. Earlier measurements[27] by Soviet scientists using rocket-borne hygrometers over Thumba show an increase in the H_2O mixing ratio from 1.6 ppmv at 20 km to about 10 ppmv at 60 km. However, it is found that these values were larger than the mid-latitude values[28] and these measurements overestimated the H_2O concentrations[29]. Recently published satellite results[30] reveal that the H_2O mixing ratio is low in the tropical lower stratosphere and increases at higher latitudes. While the larger values observed at higher latitudes are partly due to the CH_4 oxidation, the low values found over tropics are probably due to the low temperature around the tropical tropopause region[24]. The chemical, dynamical and thermodynamical processes make the behaviour of atmospheric water vapour a complex one.

Few more in situ measurements of H_2O are planned over Hyderabad. In these future experiments, measurements will be made on the absorption of solar radiation in the 950 nm region. Since the absorption of H_2O in the $\rho\sigma\tau$ band is about a factor of 4 higher than that in the 0.8 μm band, these results will be more accurate and less dependent on the derived ozone and aerosol concentration values.

Table 2—Water Vapour Mixing Ratios Obtained over Hyderabad on 22 Oct. 1985

Altitude km	Mixing ratio ppmv	Altitude km	Mixing ratio ppmv
10	6.62 ± 1.34	21	3.21 ± 0.85
11	5.02 ± 0.93	22	3.31 ± 0.85
12	4.08 ± 0.81	23	3.54 ± 0.91
13	3.53 ± 0.56	24	3.77 ± 0.96
14	3.14 ± 0.43	25	3.95 ± 1.13
15	2.92 ± 0.41	26	3.99 ± 0.86
16	2.82 ± 0.45	27	3.80 ± 0.85
17	2.84 ± 0.52	28	3.48 ± 0.83
18	2.99 ± 0.62	29	3.34 ± 0.76
19	3.03 ± 0.75	30	3.04 ± 0.64
20	3.13 ± 0.83	31	2.51 ± 0.60

Acknowledgement

The authors would like to thank Messrs Y B Acharya, J T Vinchhi and A J Shroff for the fabrication of the instrument, and the staff of the Hyderabad Balloon Facility for the successful balloon flight.

References

1 Sarkar S K, Dutta H N, Pasricha P K & Reddy B M, *Atlas of tropospheric water vapour over the Indian subcontinent* (National Physical Laboratory, New Delhi), 1982.

2 Bates D R & Nicolet M, *J Geophys Res (USA)*, **55** (1950) 301.

3 Twomey S, *Atmospheric aerosols* (Elsevier Scientific Publishing Co., New York), 1977, 68.

4 Ingels J, Nevejans D, Frederick P & Arijs E, *J Geophys Res (USA)*, **91** (1986) 4017.

5 Brewer A W, *Q J R Meteorol Soc (GB)*, **75** (1949) 351.

6 Ellsaesser H W, Harries J E, Kley D & Penndorf R, *Planet & Space Sci (GB)*, **28** (1980) 827.

7 Kley D, Schmettekopf A L, Kelly K, Winkler R H, Thompson T L & McFarland M, *Geophys Res Lett (USA)*, **9** (1982) 617.

8 Kley D & Stone E J, *Rev Sci Instrum (USA)*, **49** (1978) 691.

9 Mastenbrook H J, *J Atmos Sci (USA)*, **25** (1968) 299.

10 Khun P M, cited in *Atmospheric water vapour*, edited by A Deepak, T D Wilkerson and L H Ruhnke (Academic Press, New York), 1980, 291.

11 Tanaka M, Nakazawa T & Fukabori M, *J Quant Spectrosc & Radiat Transfer (GB)*, **28** (1982) 463.

12 Koepke P & Quenzel H, *Appl Opt (USA)*, **17** (1978) 2114.

13 Acharya Y B, Jayaraman A & Subbaraya B H, *Adv Space Res (GB)*, **5** (1985) 65.

14 Subbaraya B H, Jayaraman A, Acharya Y B, Fabian P, Borchers R & Shyam Lal, *Indian J Radio & Space Phys*, **15** (1986) 67.

15 Ackerman M, cited in *Mesospheric models and related experiments*, edited by G Fiocco (D Reidel Publishing Co., Dordrecht, Netherlands), 1971, 149.

16 Jayaraman A & Subbaraya B H, *Rocket and balloon measurements of the vertical distribution of aerosols in the tropics*, Paper presented at the IAMAP symposium on aerosols and climate, XIX General Assembly of IUGG, Vancouver, Canada, 9-22 Aug. 1987.

17 Subbaraya B H, Jayaraman A & Acharya Y B, cited in *Current Problems in Atmospheric Radiation*, edited by Giorgio Fiocco (Deepak Publishing Co., Virginia, USA), 1984.

18 Jayaraman A & Subbaraya B H, *Phys Scr (Sweden)*, **36** (1987) 358.

19 *US Standard Atmosphere*, 1976, NOAA-S/T76-1562 (Superintendent of Documents, US Government Printing Office, Washington D C), 1976.

20 Penndorf R, *J Opt Soc Am (USA)*, **47** (1957) 176.

21 Kley D, Stone E J, Handerson W R, Drummond J W, Harrop W J, Schmeltekopf A L, Thompson T L & Winkler R H, *J Atmos Sci (USA)*, **36** (1979) 2513.

22 *Atmospheric Ozone* 1985, WMO, Global Ozone Research and Monitoring Project, Rep. No. 16.

23 Fischer H, Fergg F, Rabus D & Burkert P, *J Geophys Res (USA)*, **90** (1985) 3831.

24 Brasseur G & Solomon S, *Aeronomy of the middle atmosphere* (D Reidel Publishing Co., Dordrecht, Netherlands), 1984, 227.

25 Farmer C B, Raper O F, Robbins B D, Toth R A & Mueller C, *J Geophys Res (USA)*, **85** (1980) 1621.

26 Pollock W, Heidt L E, Lueb R & Ehhalt D H, *J Geophys Res (USA)*, **85** (1980) 5555.

27 Yushov V A, *Proceedings of the Indo-Soviet symposium on space research held during* 21-26 *Feb.* 1983 (Indian Space Research Organisation, Bangalore) 1983, pp. 7.04-1 to 7.04-7.

28 Mastenbrook H J, *Can J Chem (Canada)*, **52** (1974) 1527.

29 Subbaraya B H, *Indian J Radio & Space Phys*, **16** (1987) 25.

30 *Handbook for MAP* 22, edited by J M Russell (SCOSTEP Secretariat, University of Illinois, Illinois), 1986.